Quantum wires as logic operators: XNOR and NOR gate response in a ballistic interferometer

S. Bellucci[1] and P. Onorato[1,2]
[1]*Laboratori Nazionali di Frascati, INFN, P.O. Box 13, 00044 Frascati, Italy*
[2]*Department of Physics "A. Volta," University of Pavia, Via Bassi 6, I-27100 Pavia, Italy*
(Received 8 January 2010; revised manuscript received 3 March 2010; published 20 April 2010)

We discuss the electron transport through a quantum dot formed by two quantum point contacts (QPCs) along a semiconducting quantum wire. The XNOR and NOR gate response in this system is investigated. The widths of the QPCs are modulated by lithographically patterned metallic electrodes where two gate voltages, namely, V_a and V_b, are applied. Those external voltages are treated as the two inputs of the gates. Here we calculate the conductance-energy characteristic as a function of the geometrical parameters and gate voltages. Our study suggests that, for an appropriate choice of the working Fermi energy and of the distance between the barriers, a high output current (1) (in the logical sense) appears if both of the two inputs are low (0), while if only one input is high (1), a low output current (0) results. It clearly demonstrates the XNOR gate behavior and this aspect may be utilized in designing an electronic logic gate. By changing the distance a NOR gate can be produced, where a high output current (1) appears only if both inputs are low (0), while a low output current (0) results otherwise.

DOI: 10.1103/PhysRevB.81.165427 PACS number(s): 73.50.Jt, 72.25.−b, 72.20.My

I. INTRODUCTION

In the last decades progress in semiconductor device fabrication[1] and carbon technology[2] allowed for the construction of several low-dimensional structures at the nanometric scale, and many novel transport phenomena were revealed. Thus the study of electron transport through nanometric devices has attracted a great deal of interest, both for application and research, in the field of developing charge-based nanoelectronics as well as spin-based nanoelectronics (spintronics[3]).

In recent years, the study of spintronics devices, which utilize the spin rather than the charge of an electron, has been intensified.[4,5] Many researchers proposed to use the spin degree of freedom in information processing applications where logical states are up and down with respect to certain quantization directions. Moreover the electron spin degree of freedom can also be considered one of the prospective carriers of qubits, the fundamental units in quantum information processing.[3] The realization of this aim, however, requires one to perform basic spin operations such as the production of spin-polarized carriers[6,7] and the rotation of spin orientation.[8]

On the other hand, also conventional electronic devices with micrometric and submicrometric dimensions, which rely upon the transport of electrical charge carriers, were intensively studied in the last two decades. In fact, with the aid of present technological progress, quantum systems can be used extensively in designing nanodevices, and indeed they are treated as the fundamental building blocks for future generation of nanoelectronics. In some recent papers nanometric logic gates[9,10] were proposed starting from the key idea of designing nanodevices based on the concept of the quantum interference effect.

Here, we propose a nanometric device able to rely a logic operation. Our proposal is essentially based on transport properties of quantum wires (QWs) in the ballistic (coherent) regime. The latter devices, patterned in a two-dimensional electron gas (2DEG), can be fabricated from semiconductor-based heterostructures.[11,12]

The main focus of our paper is to describe the XNOR (and NOR) gate response of an intrinsic quantum dot (IQD) embedded in a QW. The IQD is formed by two quantum point contacts (QPCs) (Ref. 1) placed at a fixed distance L along the wire. The strength of the barriers corresponding to the QPCs is modulated by the gate voltages, V_a and V_b, respectively, which are considered as the two inputs of the logic gates. The geometry of the device we are considering is reported in Fig. 1.

The gate behavior is addressed by studying the conductance-energy characteristics in terms of the geometric properties and gate voltages. The results have to be compared with the truth Tables I and II, the logic tables used in connection with Boolean algebra. In Sec. II we present the model and the basic bricks of our calculations, in Sec. III we report the main results obtained, while in Sec. IV we discuss the feasibility of the proposed devices.

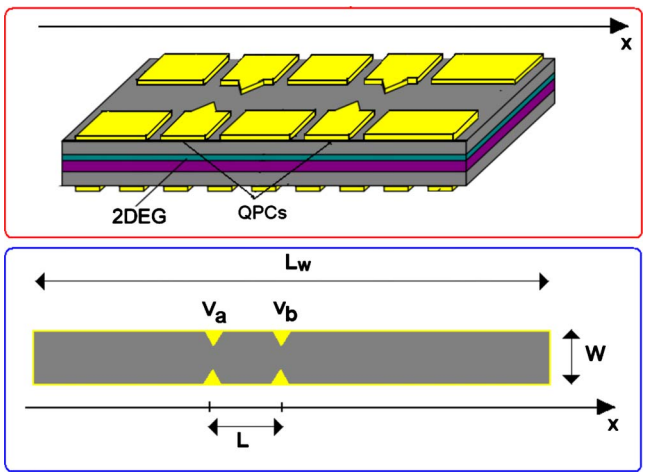

FIG. 1. (Color online) The device can be assumed as a quasi-1D wire of width W ranging between ~25 and 100 nm. Schematic plots of a quantum wire along the x axis.

TABLE I. The XNOR truth table and the corresponding gate response. The conductance G is computed at the Fermi energy $E_F \sim 1.0875\hbar\omega$ for $L=20W/(2\pi)$.

Input-I ($V_a/\hbar\omega$)	Input-II ($V_b/\hbar\omega$)	Logic response	Conductance ($2e^2/h$)	Current I/I_0
0	0	1	1	$\sim 2\times 10^{-2}$
2	0	0	~ 0.05	$\leq 2\times 10^{-3}$
0	2	0	~ 0.05	$\leq 2\times 10^{-3}$
2	2	1	~ 1	$\sim 2\times 10^{-2}$

II. MODEL AND THEORETICAL APPROACH

A. Model

Quantum wire. The ballistic one-dimensional (1D) wire is a nanometric solid-state device in which the transverse motion is quantized into discrete modes and the longitudinal motion (along x in Fig. 1) is free. In this case, electrons propagate freely down to a clean narrow pipe and electronic transport with no scattering can occur. Next we assume that the motion perpendicular to the 2DEG (along z) is quantum mechanically frozen out (i.e., with a mean value $\langle p_z\rangle=0$ in the ground state for the potential wells in the z or x direction).

Following Ref. 13, the lateral confining potential of a QW, $V_c(x)$, is approximated by a parabola

$$\hat{H}_0 = \frac{\mathbf{p}^2}{2m^*} + V_c(\mathbf{r}) = \frac{\mathbf{p}^2}{2m^*} + \frac{m^*}{2}\omega^2 y^2. \tag{1}$$

The quantity ω controls the strength (curvature) of the confining potential while the in-plane electric field is directed along the transverse direction.

It follows that the energies, in the first-order approximation, read

$$E_{n,k} = \hbar\omega\left(n+\frac{1}{2}\right) + \frac{\hbar^2}{2m^*}k^2. \tag{2}$$

Hence we can conclude that two-split channels are present for a fixed Fermi energy, E_F, corresponding to $\pm p_x$ with eigenfunctions

$$\varphi_{\varepsilon_F,n} = u_n(y)e^{ik_n(E_F)x},$$

where $u_n(y)$ are displaced harmonic oscillator eigenfunctions and

TABLE II. NOR truth table and corresponding gate response. The conductance G is computed at the Fermi energy $E_F \sim 1.0875\hbar\omega$ for $L=W/(2\pi)$.

Input-I ($V_a/\hbar\omega$)	Input-II ($V_b/\hbar\omega$)	Logic response	Conductance ($2e^2/h$)	Current I/I_0
0	0	1	1	$\sim 2\times 10^{-2}$
2	0	0	~ 0.05	$\leq 2\times 10^{-3}$
0	2	0	~ 0.05	$\leq 2\times 10^{-3}$
2	2	0	~ 0.001	~ 0

$$k_n(E_F) = \sqrt{\frac{2m^*}{\hbar^2}\left(E_F - \hbar\omega\frac{2n+1}{2}\right)}.$$

Next we limit the discussion to the lowest subband ($n=0$) and define $\varepsilon_F=E_F-\hbar\omega/2$ so that $k=\sqrt{2m^*\varepsilon_F/\hbar^2}$.

Quantum point contacts. QPCs are constrictions defined in the plane of a 2DEG with a width on the order of the electron Fermi wavelength and a length much smaller than the elastic mean-free path. QPCs proved to be very well suited for the study of quantum transport phenomena. They have been realized in split-gate devices, for example, which offer the possibility to tune the effective width of the constriction, and thus the number of occupied 1D levels, via the applied voltage.

Here we discuss the presence of two QPCs along a QW at a distance L which can be represented by a potential

$$V_B(x) = V_a\delta\left(x+\frac{L}{2}\right) + V_b\delta\left(x-\frac{L}{2}\right),$$

where $\delta(x)$ is a Dirac delta function.[14] The strength of the barriers, which shrink the 1D channel, are modulated by the input voltages, V_a and V_b.

The transmission. Starting from the model introduced above, the transmission probability can be analytically calculated by solving the Shrödinger equation in the 1D limit. When $V_a=V_b=U$, we obtain

$$\frac{1}{T} = \left\{1 + \frac{2U^2}{\varepsilon_F}\left[\cos(k_nL) - \frac{U}{\sqrt{2\varepsilon_F}}\sin(k_nL)\right]^2\right\},$$

which, in the limit of just one QPC on, becomes $1/T=[1+\frac{2U^2}{\varepsilon_F}]$. These results can be compared with those obtained in several papers in the past,[15,16] also for more realistic models of a constriction delimited by gates represented by a potential varying with both x and y.[17] As in this paper we are interested in the interference of the electron waves propagating between the QPCs, we do not need more details about the transmission of a single QPC, and the Dirac delta plays well.

B. Ballistic transport and Landauer formula

The transport properties of the submicrometric systems subject to a constant, low bias voltage (linear regime) at zero temperature are described by the Landauer formula.[18] The latter formula gives the conductance G as,

$$G = \frac{e^2}{h}\sum_{n',n=0}^{M}\sum_{\sigma',\sigma} T_{n'n}^{\sigma'\sigma}, \tag{3}$$

where $T_{n'n}^{\sigma'\sigma}$ denotes the quantum probability of transmission between incoming (n,σ) and outgoing (n',σ') asymptotic states defined on semi-infinite ballistic leads. The labels n,n' and σ,σ' refer to the corresponding mode and spin quantum numbers, respectively. In our case, where a spin-independent scattering by the barriers is considered, a factor 2 is present due to the spin degeneracy. Moreover also the sum over n is neglected since we analyze the case of just one mode involved: $n=n'=0$.

The Landauer formula in the latter case can be written as

$$G = (2e^2/h)T \tag{4}$$

and works in the ballistic transport regime, in which scattering with impurities and electron-electron interaction can be neglected and the dimensions of the sample are reduced below the mean-free path of the electrons. We also assume that this regime is not destroyed by the presence of the QPCs along the QW.

Since the Landauer formula works just at $T=0$, at finite temperature, T, a more general formulation, which takes into account the width of the distribution of injected electrons is given by[19]

$$G = -(e^2/h)\sum_{\sigma}\int_0^{\infty} d\varepsilon \frac{\partial f(\varepsilon,\varepsilon_F,T)}{\partial \varepsilon}|T_\sigma(\varepsilon_F)|^2, \tag{5}$$

where f is the Fermi distribution function and T the is temperature.

In order to evaluate the current (I) passing through the QW, as a function of the applied bias voltage (V), we can use the relation,[20]

$$I(V) = \frac{e}{\pi\hbar}\int_{E_F-eV/2}^{E_F+eV/2} T(E)dE, \tag{6}$$

where E_F is the equilibrium Fermi energy.

III. RESULTS

In order to illustrate the results, let us first mention the values of the different parameters used for the calculations. Here we have in mind conductors smaller than the dephasing length L_ϕ, i.e., a wire of length $L_W \lesssim 5$ μm for low temperatures ($T \ll 1$ °K).

The energies are given in unit

$$\hbar\omega = \frac{\hbar^2 4\pi^2}{2m^* W^2},$$

where we suppose $\hbar\omega \sim 50$ meV for $W=20$ nm and $\hbar\omega \sim 8$ meV for $W=50$ nm. The external voltages are given in units of $V_0=\hbar\omega/e$ and will be assumed as $V_{a/b}=2V_0$ which ranges from tens of milli volts to 0.1 V. These potentials correspond to an effective width of the channel near the QPCs more than 1.5 times narrower than the QW. The current unit is given by $I_0=G_0V_0$, where $G_0=2e^2/h$ is the conductance quantum so that $I_0=e\omega/\pi$ is on the order of nanoampere.

A. XNOR gate

In Fig. 2 we display the conductance-energy (G-ε_F) characteristics for the IQD patterned in the QW. Here we assume $2\pi L/W=20$, so that many interference peaks are revealed for $\varepsilon_F \lesssim \hbar\omega$, corresponding to the lowest subband. All these resonance peaks are associated with the energy eigenvalues of the IQD, and therefore, we can say that the conductance spectrum itself reveals the electronic structure of the IQD.

The latter result is emphasized in Fig. 3 where the G-ε_F characteristics are reported for the lowest subband. In Fig. 3

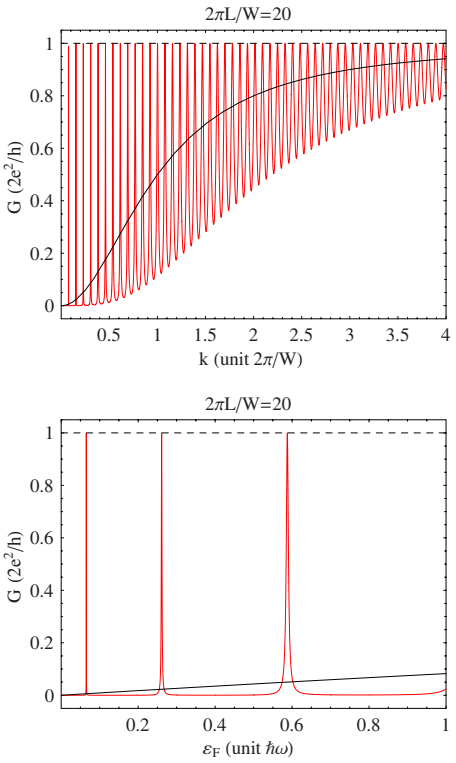

FIG. 2. (Color online) G-k and G-ε_F characteristics for a QW with two QPCs at a distance $L=(20W)/(2\pi)$. We compare the three cases of no barrier (black dashed line), one barrier (black line), and two barriers [red (dark gray) line]. The interferometric peaks due to the resonances in the IQD are shown.

the panels (a)–(d) correspond to the results for the four different combinations of the gate voltages V_a and V_b. In the particular case when $V_a=V_b=0$ i.e., both inputs are low (0), the conductance shows the maximum value $2e^2/h$ in the entire energy range [Fig. 3(a)]. This clearly indicates that the electron can conduct from the source to the drain across the QW. When $V_a=V_b=2$ [Fig. 3(d)], if we choose appropriately the working energy ε_F, the device operates near the transmission peak (at $\varepsilon_F=0.5875$ in the examined case) so that the conductance shows a value near $2e^2/h$, While, for the other two cases i.e., $V_a=2$ and $V_b=0$ [Fig. 3(b)], $V_a=0$ and $V_b=2$ [Fig. 3(c)], the conductance is substantially suppressed by the barriers ($G<0.152e^2/h$).

The results obtained near the peak observed at $\varepsilon_F \sim 0.6$ are reported in Table I and compared with the truth table of XNOR gate. The electron transmission across the QW as a function of the energies provides an important signature in the study of current-voltage (I-V) characteristics.[9,10]

All the features of electron transfer discussed in terms of conductance are also visible by studying the I-V characteristics. The current passing through the QW is computed from the integration procedure of the transmission function T as prescribed in Eq. (6). In Fig. 4 we display the I-V characteristics for the QW: (i) for the case when both inputs are zero, a high output current is obtained; (ii) in the presence of just one vanishing input, (b) and (c) cases, the current is very low (below $2\times10^{-3}I_0$); and (iii) for the case when neither of the two inputs is zero, a high output current is obtained

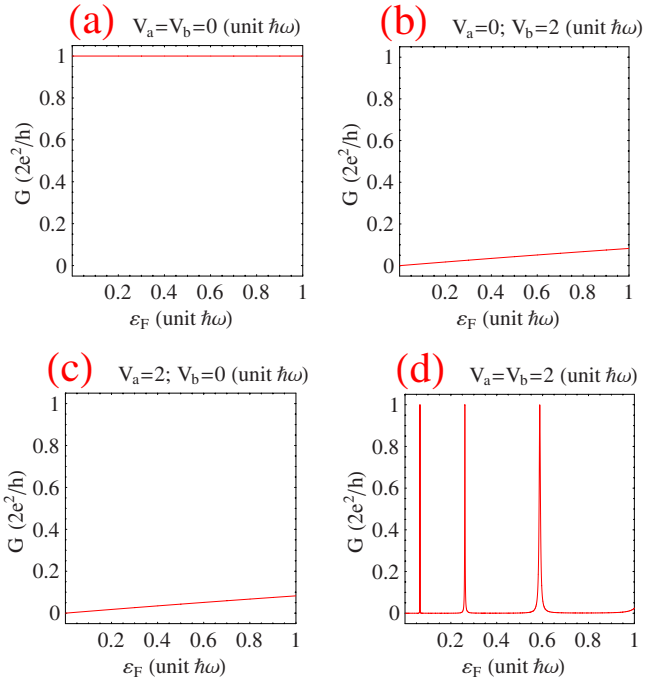

FIG. 3. (Color online) G-ε_F characteristics for a QW with two QPCs at a distance $L=(20W)/(2\pi)$. In the panels the conductance is reported in the four different cases corresponding to different voltages applied to the QPCs: (a) $V_a=V_b=0$, (b) $V_a=0$ and $V_b=2$, (c) $V_a=2$ and $V_b=0$, and (d) $V_a=V_b=2$.

$(\sim 1\times 10^{-2} I_0)$. The nonlinear characteristic in (d) is due to the existence of the sharp resonance peak in the conductance.

The bias voltage V is taken quite small (below $2\times 10^{-2} V_0$) so that the Buttiker Landauer theory can be applied. The results are also reported in Table I, where they are compared to the logical response of a XNOR gate.

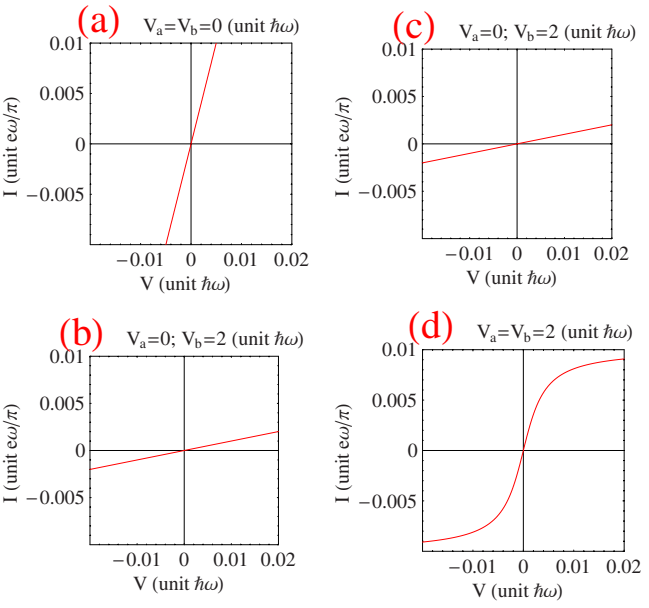

FIG. 4. (Color online) I-V characteristics for a QW with two QPCs at a distance $L=(20W)/(2\pi)$. (a) $V_a=V_b=0$, (b) $V_a=0$ and $V_b=2$, (c) $V_a=2$ and $V_b=0$, and (d) $V_a=V_b=2$.

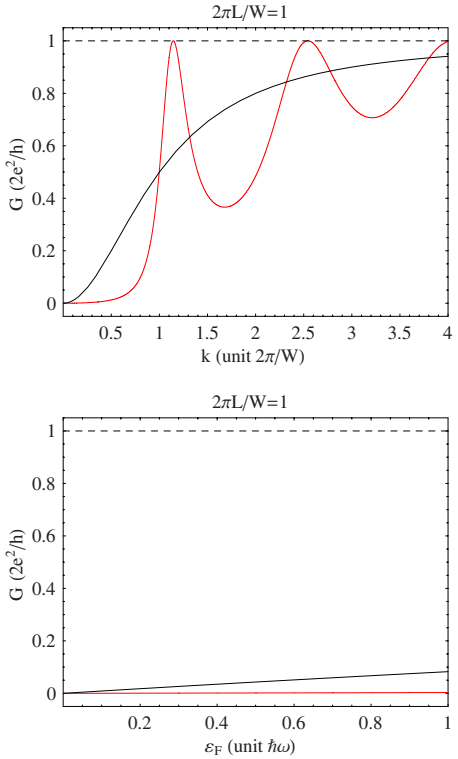

FIG. 5. (Color online) G-k and G-ε_F characteristics for a QW with two QPCs at a distance $L=(20W)/(2\pi)$. We compare the three cases of no barrier (black dashed line), one barrier (black line), and two barrier [red (dark gray) line]. The interferometric peaks due to the resonances in the IQD are shown.

B. NOR gates

In Fig. 5 we display the $(G$-$\varepsilon_F)$ characteristics for an IQD patterned in the QW. This IQD differs from the one analyzed above, because here we assume $2\pi L/W=1$, quite smaller than the previous one (20).

Now we try to figure out the dependencies of the electron transport on the input voltages in the four different cases. In Fig. 5 we display the conductance-energy $(G$-$\varepsilon_F)$ characteristics for the IQD when the two barriers are very close $(2\pi L/W=1)$. The many interference peaks (for $\varepsilon_F \leq \hbar\omega$, corresponding to the lowest subband) are now suppressed.

The conductance reported in Fig. 5 clearly indicates that a significant current is present and the conductance shows a value near $2e^2/h$ just when V_a and V_b both vanish, once we fixed the working energy $\varepsilon_F < \hbar\omega$. Hence, for the other three cases the conductance is substantially suppressed by the barriers $(G<0.1G_0)$. All features of electron transfer discussed in terms of the conductance are also visible by studying the current-voltage characteristics[9,10] reported in Fig. 6.

The results obtained are reported in Table II and compared with the truth table of the NOR gate. The nonzero value of the transmission probability is achieved only when both inputs are low (0) while a low transmission probability (0) results otherwise. This feature clearly demonstrates the NOR gate behavior.

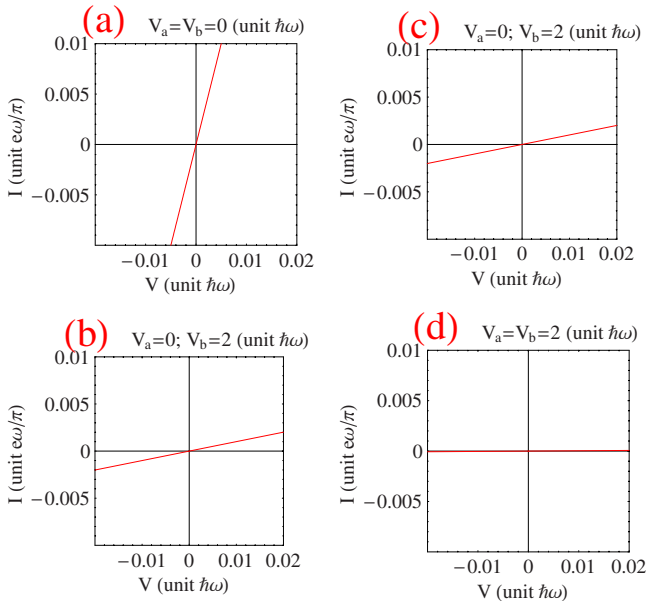

FIG. 6. (Color online) *I-V* characteristics for a QW with two QPCs at a distance $L=(W)/(2\pi)$. (a) $V_a=V_b=0$, (b) $V_a=0$ and $V_b=2$, (c) $V_a=2$ and $V_b=0$, and (d) $V_a=V_b=2$. The current unit is given by $I_0=e\omega/\pi$.

IV. DISCUSSION

In this paper we discussed two theoretical devices, capable of acting as ballistic XNOR and NOR logic gates. The devices are made of an intrinsic quantum dot formed by two quantum point contacts along a semiconducting quantum wire. The gate voltages applied to the QPCs, namely, V_a and V_b, are the two inputs of the gates.

The probability amplitude of getting an electron from the source to drain across the double QPCs depends on the combined effect of the quantum interference of the electronic waves passing through the IQD. The conductance-energy and current-voltage characteristics as functions of the geometrical parameters and input voltages were analyzed.

When the IQD is large, for an appropriate choice of the working Fermi energy, a high output current appears if both inputs are low, whereas if only one input is high, a low output current results. It clearly demonstrates the XNOR gate behavior. When the distance between the QPCs is quite small a NOR gate can be produced, where a high output current appears only if both inputs are low, while a low output current results otherwise.

Some fundamental questions have to be addressed about the feasibility of the proposed devices. All the results in this presentation are computed at absolute zero temperature, but they should be valid even for finite temperature, as the broadening of the energy levels of the QW becomes much larger than that of the thermal broadening.[20] On the other hand, in the high-temperature limit, all these features completely disappear. This is due to the fact that the phase coherence length decreases significantly with the rise of the temperature, when the contribution comes mainly from the scattering on phonons, and therefore, the quantum interference effect vanishes.

In order to estimate the values of the temperature for which the thermal broadening dominates, the energy gap $\hbar\omega$ is larger than both the Fermi energy and the thermal energy k_BT. Thus we can calculate $T_M=\hbar\omega/k_B$ which ranges between some tens to some hundreds of degree kelvin. Thus, by choosing very narrow wires, the proposed devices can easily work at room temperatures.

In this paper the finite width W of the wire was not included in the calculation. The results we have shown here were obtained using values of well width within those given by presently available 2DEGs and nanolithography techniques. In fact, the lithographical width of a wire defined in a 2DEG can be as small as 20 nm,[21] always away from the saturation region. Moreover, the lengths of the wires were assumed to be on the order of some hundreds of nanometers, i.e., distances surely available with a good precision. As we discussed in a previous paper,[22] also when 1D interacting electron systems are taken into account, the interference peaks, which the gates are based upon, are measurable.

[1] T. J. Thornton, Rep. Prog. Phys. **58**, 311 (1995).
[2] J.-C. Charlier, X. Blase, and S. Roche, Rev. Mod. Phys. **79**, 677 (2007).
[3] D. D. Awschalom, D. Loss, and N. Samarth, *Semiconductor Spintronics and Quantum Computation* (Springer, Berlin, 2008); B. E. Kane, Nature (London) **393**, 133 (1998).
[4] S. A. Wolf, D. D. Awschalom, R. A. Buhrman, J. M. Daughton, S. von Molnar, M. L. Roukes, A. Y. Chtchelkanova, and D. M. Treger, Science **294**, 1488 (2001).
[5] P. Földi, O. Kálmán, M. G. Benedict, and F. M. Peeters, Nano Lett. **8**, 2556 (2008); P. Földi, O. Kálmán, and F. M. Peeters, Phys. Rev. B **80**, 125324 (2009).
[6] F. Chi, J. Zheng, and L. L. Sun, Appl. Phys. Lett. **92**, 172104 (2008).
[7] M. Yamamoto and B. Kramer, J. Appl. Phys. **103**, 123703 (2008).
[8] S. Bellucci and P. Onorato, Phys. Rev. B **79**, 045314 (2009); **77**, 165305 (2008).
[9] S. K. Maiti, J. Phys. Soc. Jpn. **78**, 114602 (2009); Phys. Lett. A **373**, 4470 (2009).
[10] S. K. Maiti, Solid State Commun. **149**, 2146 (2009); **149**, 1623 (2009); **149**, 1684 (2009).
[11] T. Koga, J. Nitta, T. Akazaki, and H. Takayanagi, Phys. Rev. Lett. **89**, 046801 (2002).
[12] M. König, A. Tschetschetkin, E. M. Hankiewicz, J. Sinova, V. Hock, V. Daumer, M. Schäfer, C. R. Becker, H. Buhmann, and L. W. Molenkamp, Phys. Rev. Lett. **96**, 076804 (2006).
[13] S. E. Laux, D. J. Frank, and F. Stern, Surf. Sci. **196**, 101 (1988); H. Drexler, W. Hansen, S. Manus, J. P. Kotthaus, M. Holland, and S. P. Beaumont, Phys. Rev. B **49**, 14074 (1994); B. Kardynał, C. H. W. Barnes, E. H. Linfield, D. A. Ritchie, J. T. Nicholls, K. M. Brown, G. A. C. Jones, and M. Pepper, *ibid.* **55**,

R1966 (1997).

[14] The Dirac delta function is usually taken into account in order to modelize the QPCs, while any other function localized near $y=0$ can be used, see Refs. 15 and 17.

[15] See, for a review, H. van Houten and C. W. J. Beenakker, Phys. Today **49** (7), 22 (1996); C. W. J. Beenakker and H. van Houten, in Solid State Physics, edited by H. Ehrenreich and D. Turnbull (Academic, New York, 1991), Vol. 44, p. 1.

[16] V. Marigliano Ramaglia, F. Ventriglia, and G. P. Zucchelli, Phys. Rev. B **52**, 8372 (1995); V. Marigliano Ramaglia, A. Tagliacozzo, F. Ventriglia, and G. P. Zucchelli, *ibid.* **43**, 2201 (1991).

[17] M. Büttiker, Phys. Rev. B **41**, 7906 (1990). The saddle-point potential proposed here is useful to explain the backscattering suppression in the presence of a magnetic field.

[18] R. Landauer, IBM J. Res. Dev. **1**, 223 (1957); Philos. Mag. **21**, 863 (1970).

[19] R. Citro, F. Romeo, and M. Marinaro, Phys. Rev. B **74**, 115329 (2006).

[20] S. Datta, *Quantum Transport: Atom to Transistor*, 2nd ed. (Cambridge University Press, Cambridge, England, 2005).

[21] M. Knop, M. Richter, R. Maßmann, U. Wieser, U. Kunze, D. Reuter, C. Riedesel, and A. D. Wieck, Semicond. Sci. Technol. **20**, 814 (2005).

[22] S. Bellucci and P. Onorato, Eur. Phys. J. B **47**, 385 (2005).